Discovery of Small Molecule PARKIN Activator as Therapeutics for PD: An in-silico Repurposing Approach

Abdulwasiu Ibrahim (ibrahimabdulwasiu44@gmail.com)
University of Ibadan College of Medicine https://orcid.org/0000-0003-3456-005X
Nureni Ipinloju
Adekunle Ajasin University
Sulieman Alhaji Muhammad
Usmanu Danfodiyo University Faculty of Science
Oluwatoba Emmanuel Oyeneyin
Adekunle Ajasin University
Nkechi Hope Atasie
Nigerian Prisons Service

Research Article

Keywords: Drug repurposing, Parkinson's disease, Antipsychotic drugs, Anti-neuropsychiatric drugs, PARKIN, Computational approach

Posted Date: October 4th, 2022

DOI: https://doi.org/10.21203/rs.3.rs-2035291/v1

Version of Record: A version of this preprint was published at Applied Biochemistry and Biotechnology on February 3rd, 2023. See the published version at https://doi.org/10.1007/s12010-023-04376-2.

Abstract

Background

Although there is presently no cure for Parkinson's disease (PD), the available therapies are only able to lessen symptoms and preserve the quality of life. Around 10 million people globally had PD as of 2020. The widely used standard drug has recently been revealed to have several negative effects. Additionally, there is a dearth of innovative compounds entering the market as a result of subpar ADMET characteristics. Drug repurposing provides a chance to reenergize the sluggish drug discovery process by identifying new applications for already-approved medications. As this strategy offers a practical way to speed up the process of developing alternative medications for PD. This study used a computer-aided technique to select therapeutic agent(s) from FDA-approved neuropsychiatric/psychotic drugs that can be adopted in the treatment of Parkinson's disease.

Method

In the current work, a computational approach via molecular docking, density functional theory (DFT), and pharmacokinetics were used to identify possible (anti)neuropsychiatric/psychotic medications for the treatment of PD. By using molecular docking, about eight (anti)neuropsychiatric/psychotic medications were tested against PARKIN, a key protein in PD

Result

Based on the docking score, the best ligand in the trial was determined. The top hits were compared to the reference ligand levodopa (L-DOPA). A large proportion of the drugs displayed binding affinity that was relatively higher than L-DOPA. Also, DFT analysis confirms the ligand-receptor interactions and the molecular charges transfer. All the compounds were found to obey Lipinski's rule with acceptable pharmacokinetic properties.

Conclusion

The current study has revealed the effectiveness of antineuropsychiatric/antipsychotic drugs against PARKIN in the treatment of PD and lumateperone was revealed to be the most promising candidate interacting with PARKIN.

1.0 Introduction

Parkinson's disease (PD) is the most recurrent cause of the neuro-degeneration disorder, after Alzheimer's disease. It is a persistent mobility disorder with progression. Clinical symptoms, neurological signs, and brain imaging serve as the main diagnostic criteria for Parkinson's disease (PD) [1]. Dopaminergic neuronal loss in the substantia nigra of the midbrain causes striatal dopamine deficit, which reacts to Parkinson's disease (PD) movement symptoms [2]. Numerous genes, including SNCA and PARKIN, as well as the form of PD that is induced by the environment, have been linked to the disease [3, 4]. As a result, only about 10–15% of PD incidences are familial, making the majority of PD incidences random [5]. Additionally, the Parkin gene shows mutations in 50% of all autosomal recessive familial or juvenile cases, 40% of early-onset cases, and close to 15% of sporadic cases [6]. In fact, the Parkin gene is the second most common genetic cause of Parkinson's disease [7]. They manifest clinically as early and late parkinsonism in both early-onset familiar and sporadic types of Parkinson's disease (PD).

Numerous functions, including receptor trafficking and mitochondrial quality control, have been suggested to be regulated by parkin. Deletions, insertions, and point mutations are among the alterations that typically result in the loss of parkin's catalytic activity [7–9]. Parkin is vulnerable to oxidative and nitrosative assault due to its cysteine concentration, in addition to mutations affecting its function. Parkin function is lost as a result of S-nitrosylation, oxidative, dopaminergic, and stress-induced kinase phosphorylation. Currently, L-DOPA and other commercially available medications used to treat the symptoms of PD have been linked to PD patients' s dyskinesia, edema, and impulse control issues [10]. In the upcoming decades, there may be a sharp rise in the prevalence of PD patients as a result of the absence of effective treatments for the condition. Due to these drawbacks, researchers are constantly looking for novel medications with fewer negative effects. There are less than 30 therapeutic agents in both phase II and phase III clinical trials for the treatment of PD in the last few years [11]. In contrast, there are about 2000 candidate cancer therapies [12].

Drug repurposing is the method of determining if an existing medication can serve a new therapeutic purpose. Many therapies, including those for cancer, cardiovascular disease, irritable bowel syndrome, erectile dysfunction, obesity, smoking cessation, psychosis, attention deficit disorder, Alzheimer's disease, and even Parkinson's disease, have already used drug repurposing [13]. The benefits of using pre-existing drug compounds are that they reduce the need for early clinical trials that involve chemical optimization, in vitro and in vivo screening, toxicological research, bulk manufacturing, and formulation development. In contrast, it costs billions of dollars and at least 15 years for a new medication candidate to reach the market [14].

To screen eight FDA-approved antineuropsychiatric/antipsychotic medicines against parkin for the treatment of Parkinson's disease, a computational strategy utilising molecular docking, density functional theory and pharmacokinetics analysis were adopted.

2.0 Methodology

2.1 Protein preparation and *Receptor grid generation*

PARKIN (5C9V), the target protein, had an X-ray crystallographic structure that was retrieved from the Protein Data Bank (PDB). Prior to molecular docking, the protein structure was prepared using the "Protein Preparation module" process of the Maestro interface in the Schrodinger suite 2018 [15, 16]. To do this, hydrogen atoms were added to the protein, bond ordering was set, and superfluous water molecules were eliminated. Disulphide bonds were formed, missing atoms were replaced, side chains were added, and partial charges were assigned. To save energy, the OPLS3 (Optimized Potentials for Liquid Simulations) force field was used. Because the downloaded protein was co-crystallized, the ligand binding site was used to identify the active site. Receptor grid generation workflow was used to define a grid (box) around the ligand, to keep all the functional residues in the grid [17].

2.2 Ligand preparation

Eight FDA-approved antineuropsychiatric/antipsychotic medications were chosen based on literature research, and their 3D structures were retrieved from the PubChem database. The ligands were pre-processed by LigPrep, which included the generation of tautomers and ionisation states at pH 7.0 2.0. Epik was then used to add hydrogen atoms, neutralise charged groups, and optimise the shape of the ligands [15, 18].

2.3 Molecular docking

Extra-precise (XP) docking was done using the produced protein and ligands using the Maestro interface's ligand-docking method in the Schrodinger suite of 2018. Different conformations were produced by maintaining the flexibility of the ligand structures. These computations were carried out using the OPLS force field [19].

2.4 Density Functional theory

Quantum Chemical Calculation

Quantum chemical calculations are employed to predict the structure and distribution of electronic density of the FDA-approved drug and their electron transfer to the receptor. Density functional theory (DFT) is a very popular way of evaluating the chemical reactivity of molecules [20, 21]. Quantum chemical calculations were performed on the structures of the 8 FDA-approved drugs using Spartan 14 computational software [22, 23] on an Intel (R) computer with 6.00 GB ram specifications, 500G hard disc and 2.60GHz software package. The 3D structure in SDF format of all the compounds was downloaded from pubchem database. The 3D structures were imported into Spartan 14 software for geometry optimization. A conformation distribution search was run on each compound and the most stable conformer was picked for geometric optimization. Optimization of the structure of the phytochemicals was done using the exchange correlation hybrid functional B3LYP [24, 25] and 6–31* basis set [26] in a vacuum. The quantum parameters calculated include; frontier molecular orbitals energy (FMOs), that is, the energy of the highest occupied molecular orbital (E_{HOMO}) and energy of the lowest unoccupied molecular orbital (E_{LUMO}). Other vital parameters such as energy band gap, Eg (Eq. (1)), ionization energy, I (Eq. (2)), electron affinity, A (Eq. (3)) electronegativity, χ (Eq. (4)), chemical potential, μ (Eq. (5)), chemical hardness, η (Eq. (6)), chemical softness, δ (Eq. (7)) and global electrophilicity index, ω (Eq. (7)), electron-donating power ω^- (Eq. (9)) and electron accepting power, ω^+ (Eq. (10)) were calculated according to Koopman's theorem [27].

$Eg = E_{LUMO} - E_{HOMO}$ 1

$I = -E_{HOMO}$ 2

$A = -E_{LUMO}$ 3

$\chi = \frac{I+A}{2}$ 4

$\mu = -\chi$ 5

$\eta = \frac{I-A}{2}$ 6

$\delta = \frac{1}{\eta}$ 7

$\omega = \frac{(E_{LUMO}+E_{HOMO})^2}{4(E_{LUMO}-E_{HOMO})}$ 8

$\omega^- = \frac{(3E_{HOMO}-E_{LUMO})^2}{16\eta}$ 9

$\omega^+ = \frac{(E_{HOMO}+3E_{LUMO})^2}{16\eta}$ 10

2.5 Drug-likeness Properties

The test compounds' drug-likeness properties were evaluated using the SwiessADME web server (http://www.swissadme.ch/) following Lipinski's rule of five (MW 389 500; HBA 10, HBD 5, iLogP 5, and TPSA 120).

2.6 In silico Pharmacokinetics

Using the admetSAR online server (admetSAR (ecust.edu.cn), the test drugs' absorption, distribution, metabolism, excretion, and toxicity (ADMET) characteristics were evaluated.

3.0 Results And Discussion

3.1 Molecular docking

De novo drug design and development have encountered several serious challenges in recent years as a result of its expense and duration. While investment in the pharmaceutical industry has increased, the number of new therapeutic agents that have been approved has remained constant; as a result, computer-aided drug repurposing is an effective and motivating tool for coming up with new applications for therapeutic agents that have already been developed. There are numerous instances of medications that have been repurposed after being found by a computer model and used to treat various ailments. An excellent illustration is the use of Raltegravir, once an HIV-1 integrase inhibitor, as adjuvant therapy in cancer [28], and the use of Valsartan, formerly an angiotensin receptor blocker, for Alzheimer's disease [29].

However, the main focus of this computational study was to identify specific therapeutic agent(s) from FDA-approved neuropsychiatric/psychotic drugs that could serve as promising agents in the treatment of juvenile Parkinson's disease.

Eight FDA-approved drugs from the named class were screened at the known binding site of the PARKIN crystal structure in order to find promising therapeutic agents with high binding affinities against the active site of PARKIN. The binding energies of these drugs were calculated using extra precision (XP) docking. Excellent binding affinity is indicated by a low docking score. In the specific binding pocket of PARKIN, the molecular docking scores of the tested ligands vary from − 5.845 kcal/mol to -2.658 kcal/mol (Fig. 1). Additionally, the co-crystallized ligand's redocking with an RMSD value of 0.90 supports the validity of the docking approach. In the docking result, six of the screened ligands were shown to be effective namely Lumateperone (CID: 21302490), Anisoperidone (CID: 19104), Melperone (CID: 15387), Bromperidol (CID: 2448), Azabuperone (CID: 18484), Deutetrabenazine (CID: 73437646), could be manifest as an excellent putative and selective inhibitor of PARKIN than reference ligand (L-DOPA; CID: 6047) as determined by their relatively high binding energy score. Following the visualization of PARKIN active site with the co-crystalized ligand, the following essential amino acid residue SER 167, ARG 170, MET 192, ARG 191, ASM 190, PRO 189, ILE 188, LEU 187, VAL 186, ALA 206, GLU 207, PHE 208, ASP185, TRP 183, PHE 209, PHE 210, THR 222, SER 223, VAL 224, ALA225, LEU 226, MET, 227, GLU 300, HIS 302 were revealed to play a pivotal role in PARKIN-ligand interaction. These amino acid residues play a fundamental role in forecasting PARKIN binding sites and their mechanism of catalysis. The docked compounds interact with GLU 207, PHE 210, PHE 208, ALA225, LEU 187, ASN 190, SER 223, ARG 170. Practically, the ligand-PARKIN interaction results in inter/intramolecular forces of interaction such as hydrogen bonding, pi-pi stacking, pi-cation, and salt bridge through hydrogen bond formation with the nitrogen and oxygen atom of the numerous ring and Van der Waals interactions (Table 1). In this study, Fig. 1 represent the docking score where **Lumateperone** is the best molecule against PARKIN, with the highest binding score of **− 5.845kcal/mol**, followed by **Anisoperidone − 5.517Kcal/mol**.

Remarkably, all the docked complexes, as well as the reference ligand (L-DOPA), were observed for additional molecular interaction profiling, including hydrogen, hydrophobic, polar, charged positive and negative, and glycine interactions suggesting the prime role of intermolecular interaction in the stability and better binding orientation of the respective docked complexes.

3.2 Quantum Chemical Calculations

Density functional theory (DFT) is the most widely and popular quantum theory used for the calculation of the electronic structure of molecules. In drug design, DFT is employed to study the electronic parameters of isolated drug molecules, provide an understanding of chemical reactivity and investigate drug-enzyme interactions. The results of all the chemical reactivity properties of the 8 FDA-approved drugs are shown in Table 2. Frontier molecular orbitals (FMOs) are employed to explain many reactions system. The FMOs locate the area of chemical bonds that are chemically reactive. This has been used for describing the chemical reactivity and stability of small molecules [30–32]. Highest occupied molecular orbital (HOMO) and lowest unoccupied molecular orbital (LUMO) are the two most important molecular orbitals in a molecule. The energy of HOMO (E_{HOMO}) and LUMO (E_{LUMO}) explains the type of donor-acceptor interaction of electrons in a molecular system. The E_{HOMO} and E_{LUMO} are used to study the potential of organic compounds against target receptors. E_{LUMO} describes the electron-donating ability of a molecule while E_{LUMO} explains the electron-accepting ability of a molecule. High E_{HOMO} and low E_{LUMO} values signify the great potential of a molecule to donate and accept electrons readily [30–32]. From Table 2, it was observed that lumateperone had a higher value of E_{HOMO} (-4.47 eV) than other compounds. These predictions from E_{HOMO} suggest that lumateperone will have greater facility towards electron donation therefore highest inhibition potential with the target enzyme than other studied compounds. Also, tafamidis had the lowest E_{LUMO} indicating the compound that can accept electrons readily among others. Furthermore, the energy bang gap (Eg), which is the difference between E_{LUMO} and E_{HOMO}, plays an important role in explicating the chemical reactivity and stability of a molecule. High band gap energy usually signifies greater stability while low band gap energy signifies high reactivity. As shown in Table 2, Lumateperone had the lowest band gap energy (3.13 eV). This indicates the most chemically reactive molecule among all others. lumateperone will have the highest inhibition efficiency with the target enzyme than others.

Ionization energy (I) is the energy required to remove the most loosely bonded electrons from their orbital in an atom or molecule. The higher ionization energy of a molecule indicates that the energy needed to remove its valence electron will be high and hence, high stability of the molecule. Lower the ionization energy, the higher the reactivity and vice versa [33]. Table 2 shows the pattern of increase in ionization potential, which follows the pattern of increase of E_{HOMO}. Lumateperone displayed the lowest ionization energy and therefore, the most reactive among others.

Electronegativity (χ) is a property that explains the ability of an atom, group of atoms or functional group to attract an electron toward itself [34]. Tafamidis displayed the highest electronegativity value (4.50 eV). The high electronegativity of this compound can be related to the presence of 2-chlorine atoms attached to phenyl moiety on the ring.

The electronic chemical potential (μ) measures the releasing propensity of an electron from the equilibrium system. Lumateperone had the highest chemical potential (-2.90 eV)

Global hardness (η) measures the resistance to charge transfer and global softness (δ) measures the molecule's capability to charge transfer. These properties have been used in the establishment of chemical processes [35]. Lumateperone had the lowest hardness (1.57 eV) and the highest softness (0.64 eV) indicating the best compound susceptible to charge transfer and therefore the most reactive compound.

The electrophilicity index (ω) measures the potential of a molecule to take up electrons. It explains the stabilization energy of the molecule when saturated by electrons coming near the environment [34]. Electron-donating power (ω^-) and electron-accepting power (ω^+) are used to measure the donor-acceptor interactions. Highly effective electron donors have lower values of electron-donating ability and vice versa. Also, highly effective electron acceptors have a higher value of electron-accepting power. Lumateperone had the lowest electron-donating power (5.82 eV) indicating the best electron donor while tafamidis had the highest electron accepting power.

3.3 HOMO and LUMO orbital surfaces

The HOMO and LUMO orbital surfaces are shown in Table 3. Lumateperone had HOMO orbitals spread over benzopyrazine ring which can be attributed to the presence of a pyrazine ring containing nitrogen atoms that can enter donor-acceptor interactions and release an electron from its lone pair. The LUMO orbital surface spread over the flourophenylpropanone. Anisoperidone had HOMO surface disperse over the phenylpyridnyl ring while the LUMO orbital disperse over the methoxylphenyl ring. In melperone, the LUMO orbital spread over the nitrogen atom in piperidinyl ring attached to the structure. The electron-withdrawing potential of fluorine attached to the structure enables LUMO orbital to shift and disperse over flourophenyl ring in the structure. Bromperidol, Azabuperone and pimozide had HOMO orbital spread over the nitrogen-containing phenyl ring while the LUMO orbital spread over the fluorine-containing phenyl ring. The HOMO and LUMO orbital of tafamidis spread over the ring.

Table 2
Reactivity descriptors of the studied compounds computed

Comp	E_{HOMO}	E_{LUMO}	Eg	I	A	χ	μ	η	δ	ω	ω^-	ω^+
Lumateperone	-4.47	-1.34	3.13	4.47	1.34	2.90	-2.90	1.57	0.64	2.70	5.82	2.88
Anisoperidone	-5.58	-1	4.58	5.58	1	3.29	-3.29	2.30	0.44	2.37	6.77	2.01
Melperone	-6.02	-1.41	4.61	6.02	1.41	3.71	-3.71	2.31	0.43	3.00	7.52	2.85
Bromperidol	-5.91	-1.49	4.42	5.91	1.49	3.70	-3.70	2.21	0.45	3.10	7.45	3.05
Azabuperone	-5.89	-1.46	4.43	5.89	1.46	3.67	-3.67	2.22	0.45	3.05	7.41	2.98
Deutetrabenazine	-6.01	-0.42	5.59	6.01	0.42	3.21	-3.21	2.80	0.38	1.85	6.93	1.18
Pimozide	-5.59	-0.45	5.14	5.59	0.45	3.02	-3.02	2.57	0.39	1.77	6.47	1.17
Tafamidis	-6.69	-2.32	4.37	6.69	2.32	4.50	-4.50	2.19	0.48	4.64	9.01	5.33

3.4 Molecular Electrostatic Potential Analysis

Molecular electrostatic potentials (MEPs) provide well information on the chemical/biological reactivity of a molecule. The 3D spatial distribution of the electrostatic potential is responsible for the binding of a ligand to the active site of an enzyme. The MEP map displays the most likely site for nucleophilic and electrophilic attacks. The MEPs are represented by color scheme. Red and blue regions represent partially negative charge (electron-rich) and partially positive charge (electron deficient) while yellow, light blue and green regions represent slightly electron-rich, slightly electron-deficient and neutral. The MEP map for all the compounds are shown in Fig. 2. As seen from the table N, O, F, Cl and carbon atoms in aromatic phenyl ring in all the compounds display the most negative and partial negative electrostatic potential indicating the potential site for electrophilic attacks. Also, all hydrogen atoms display positive electrostatic potential.

3.5 Mulliken charge distribution (MCD) analysis

The electronic charges play an important role in determining the bonding ability of a molecule. It is useful in understanding the charge distribution in a molecule. Mulliken charge values for the constituent atoms of the studied compounds are presented in Table 4. The carbon atom directly attached to the electronegative element displayed the maximum positive atomic charges in all the compounds. In Lumateperone, O1, N1, N2 and N3 displayed the maximum negative atomic charge while C13, C22 and C28 showed the maximum positive atomic charge. Anisoperidone had the highest negative atomic charge at O0, O1 and N2 while the maximum positive atomic charges are located at C12 and C23. C9, O1 and N2 had the maximum negative atomic charge in Melperone and the maximum positive charges are found at C12 and C18. Furthermore, Bromperidol had the highest negative atomic charge at O3 and N4 and the positive atomic charges can be seen at C18 and C25. Azabuperone had maximum positive and negative atomic charges at O1, C5 and C18 In Deutetrabenazine, s maximum negative atomic charges can be found at O0, O1 and 02 while the highest positive atomic charge is centered around C10, C19 and C20. Pimozide and tafamidis had the highest negative atomic charges at 02 and N5.

Table 4
Selected Mulliken Charge Distribution

Atomic charges	Mulliken Lumate-Perone	Mulliken Anisop-eridone	Mulliken Melperone	Mulliken Bromp-eridol	Mulliken Azabu-perone	Mulliken Deutetr-abenazine	Mulliken Pimozide	Mulliken Tafamidis
F0	-0.291	-	-0.292	-	-0.291	-	-0.3	
O0		**-0.506**	-	-	-	**-0.452**	-	
O1	**-0.498**	**-0.503**	-0.473	-	**-0.473**	**-0.53**	-	
F1	-	-	-	-0.288	-	-	9-0.298	
Cl0							99	0.005
Cl1								+ 0.003
Bro	-	-	-	-0.088	-	-	-	
O2	-	-	-	-0.65	-	**-0.531**	**-0.538**	**-0.528**
O3	-	-	-	**-0.498**	-	-	-	-0.584
04	-	-	-	-		-		-0.473
N2	**-0.511**	**-0.407**	**-0.399**	-	-0.391	-	-	-
N3	**-0.413**	-	-	-	-0.408	-0.432	-0.4	-
N4	**-0.505**	-	-	**-0.415**		-	-0.459	-
N5	-	-	-	-			**-0.769**	**-0.541**
C3	-	-0.133	-0.077	-		-	-	-
C4	-	-0.108	-0.264	-	-0.291	-0.017	-	-
C5	+ 0.042	-0.337	-0.26	+ 0.283	**-0.473**	-0.176	-	-
C6	-0.208	-0.156	-0.123	-0.266	-0.391	-0.127	+ 0.011	+ 0.341
C7	-0.281	+ 0.123	-0.128	-0.302	-0.408	-0.338	-0.271	+ 0.267
C8	-0.127	-0.275	-0.118	-0.121	+ 0.023	-0.133	-0.274	**+ 0.503**
C9	+ 0.088	-0.195	**-0.444**	-0.127	-0.293	+ 0.1	-0.125	+ 0.064
C10	+ 0.245	-0.339	-0.286	-0.108	-0.138	**+ 0.437**	-0.132	-0.218
C11	-0.117	+ 0.111	-0.332	0.136	-0.139	-0.252	-0.115	-0.173
C12	-0.138	**+ 0.437**	**+ 0.386**	-0.278	-0.292	-0.334	-0.288	+ 0.047
C13	**0.358**	-0.19	+ 0.058	-0.186	-0.131	+ 0.124	+ 0.34	-0.173
C14	-0.135	-0.179	-0.189	-0.187	-0.13	-0.073	-0.251	-0.155
C15	-0.108	+ 0.084	-0.155	-0.341	-0.117	-0.247	**+ 0.771**	-0.148
C16	-0.225	-0.136	-0.213	-0.154	-0.287	-0.259	-0.267	-0.076
C17	-0.216	-0.134	-0.2	-0.145	-0.334	-0.448	+ 0.349	-0.076
C18	-0.142	-0.129	**+ 0.391**	**+ 0.443**	**+ 0.387**	-0.445	-0.186	-0.12
C19	-0.277	-0.188	-	+ 0.012	0.058	**+ 0.324**	+ 0.167	**+ 0.547**
C20	-0.306	-0.163	-	+ 0.072	-0.191	**+ 0.335**	+ 0.172	-
C21	-0.341	-0.182	-	-0.173	-	-0.216	-0.182	-
C22	**+ 0.445**	-0.2	-	-0.165	-	-0.217	-0.148	-
C23	+ 0.073	**+ 0.382**	-	-0.205	-	-	-0.146	-
C24	-0.16	-0.221	-	-0.204	-	-	-0.18	-
C25	-0.175	-	-	**+0.391**	-	-	-0.185	-
C26	-0.199	-	-	-	-	-	-0.191	-
C27	-0.207	-	-	-	-	-	-0.193	-

Atomic charges	Mulliken Lumate-Perone	Mulliken Anisop-eridone	Mulliken Melperone	Mulliken Bromp-eridol	Mulliken Azabu-perone	Mulliken Deutetr-abenazine	Mulliken Pimozide	Mulliken Tafamidis
C28	**+ 0.389**	-	-	-	-	-	-0.199	-
C29	-	-	-	-	-	-	-0.193	-
C30	-	-	-	-	-	-	-0.197	-
C31	-	-	-	-	-	-	-0.2	-
C32	-	-	-	-	-	-	0.377	-
C33	-	-	-	-	-	-	0.377	-

3.6 Drug-likeness Properties

swiessADME webserver the drug-likeness properties of the screened compounds were predicted based on Lipinski's rule of five to examine the features of the compounds as drug or non-drug like and the result is provided in Table 5 below. The pharmacological and pharmacodynamics model of the compounds were assayed to predict their biological role. The rule of five (ROF) proposed by Christopher Lipinski was employed to determine their pharmacological potency via molecular weight < 500, number of HB acceptors < 10, number of HB donors < 5, and Lipohilicity (iLog p < 5). From the result obtained (Table 5) all the screened compounds were observed to have a molecular weight ranging from 197.19 to 461.55, hydrogen bond acceptor and donor ranging from 3 to 5 and 0 to 4, respectively. Topological polar surface area ranges from 103.78 to 20.31 and Lipohilicity from 0.78 to 4.23. In this regard, all the screened compounds obey the rule of five without violation of any of Lipinski's parameters.

Table 5
Drug-likeness properties of the screened compounds

Ligands	MW	H-Acceptor	H-donor	TPSA	iLogP	Violation
Tafamids	308.12	4	1	63.33	2.65	0 of 5
Leumateprone	393.5	3	0	26.79	3.68	0 of 5
Bromperidol	420.32	4	1	40.54	3.7	0 of 5
L-DOPA	197.19	5	4	103.78	0.78	0 of 5
Meloperone	263.35	3	0	20.31	3.18	0 of 5
Pimozide	461.55	4	1	41.3	4.23	0 of 5
Azabuperone	290.38	4	0	23.55	3.23	0 of 5
Anisolpirol	335.44	3	0	29.54	3.78	0 of 5
Deuterabenazine	323.46	4	0	38.77	3.47	0 of 5

3.7 Pharmacokinetics

Pharmacokinetics is determined by the drug candidate's molecular description. Prediction of absorption, distribution, metabolism, excretion, and toxicity (ADMET) features in silico has become significant in drug selection and determining its success for human therapeutic usage. As a result, these physiochemical descriptors were tested in order to establish the ADMET characteristics of the compounds utilizing the admetSAR sever. Tafamids, Bromperidol, L-DOPA, and pimozide were found to be effective and show low absorption while Leumateprone, meloperone, azabuperone, anisolpirol, and deuterabenazine show high absorption in the intestine via Caco-2 permeability, probably admissible by their molecular size. However, all the screened ligands displayed high intestinal absorption (Table 6). The result of the ADMET properties revealed that all tested ligands had a blood-brain barrier (BBB) permeability except L-DOPA. Tafamids, Bromperidol, L-DOPA, and anisolpirol are non-substrate of p-glycoprotein (P-GB) permeability while on the other hand Leumateprone, meloperone, azabuperone, pimozide, and deuterabenazine are substrates of P-glycoprotein permeability. Plasma binding protein is a biomarker for determining the binding of drugs to the proteins within the blood [36]. A drug's efficiency is primarily determined by the rate at which it binds. A low plasma protein binding rate is associated with greater efficiency and ease of diffusion [37]. Because all of the drugs have a high plasma protein binding rate, their migration to the site of action where they exert pharmacological effects may be hampered. Although, L-DOPA and meloperone displayed a moderate plasma protein binding rate.

Cytochrome P450s (CYPs) are an enzyme superfamily that plays an important role in drug metabolism [38]. According to the drug metabolism interaction, investigated compounds and L-DOPA are non-inhibitors of CYP2C19, CYP2C9, and CYP3A4, Bromperidol and pimozide are inhibitors of CYP3A4. Additionally, Tafamids, Leumateprone, meloperone, pimozide are inhibitors of CYP1A2 while all compounds except Tafamids and L-DOPA are inhibitors of CYP2D6. None of the compounds are substrates of CYP2C9. Tafamids and L-DOPA are non-substrates of CYP2D6 and CYP3A4 while Leumateprone, meloperone, azabuperone, pimozide, and deuterabenazine, Bromperidol, and anisolpirol are found potential substrate for CYP2D6 and CYP3A4.

Acute oral toxicity refers to the potential side effects of medication delivery by mouth [39]. All of the chemicals examined had low oral toxicity. The AMES test (Salmonella typhimurium reverse mutation assay) is a pharmacological screening technique that uses genetic mutation induction to assess the

carcinogenicity of a medicinal medication [40]. In the AMES test, all chemicals except L-DOPA were shown to be non-toxic. Tafamids and deuterabenazine are nephrotoxic while all compounds except deuterabenazine are non-hepatotoxic. Also, all the compounds were observed to be toxic to reproductive organ and only Tafamids is toxic to the respiratory organ (Table 6). To obtain better pharmacological molecules with a good biosafety profile, the compounds may be subjected to functional group alteration. Medication solubility has been regarded as an ultimate advantage in the drug development process because it aids in determining the drug concentration in the systemic circle, resulting in a maximal optimum response [41]. All the compounds had high aqueous solubility, which might be attributable to their high hydroxyl group count. Human Ether-a-go-go Related Gene (hERG) is a potassium channel that regulates cardiac excitability and maintains appropriate cardiac rhythm [42]. Leumateprone, anisolpirol, pimozide, and deuterabenazine, are inhibitors of hERG gene. However, Tafamids, L-DOPA, Bromperidol, azabuperone, and meloperone are non-inhibitors of the hERG gene, which confirms they would not contribute to drug-induced proarrhythmia.

Table 6
Pharmacokinetics properties of the screened ligand

Models	Tafamids	Leumateprone	Bromperidol	L-DOPA	Meloperone	Pimozide	Azabuperone	Anisolpirol	Deuterab
Ames mutagenesis	-	-	-	+	-	-	-	-	-
Acute Oral Toxicity (c)	II	III	II	III	III	III	III	III	III
Blood Brain Barrier	+	+	+	-	+	+	+	+	+
Biodegradation	-	-	-	-	-	-	-	-	-
Caco-2	-	+	-	-	+	-	+	+	+
Carcinogenicity (binary)	-	-	-	-	-	-	-	-	-
CYP1A2 inhibition	+	+	-	-	+	+	-	-	-
CYP2C19 inhibition	-	-	-	-	-	-	-	-	-
CYP2C9 inhibition	-	-	-	-	-	-	-	-	-
CYP2C9 substrate	-	-	-	-	-	-	-	-	-
CYP2D6 inhibition	-	+	+	-	+	+	+	+	+
CYP2D6 substrate	-	+	+	-	+	+	+	+	+
CYP3A4 inhibition	-	-	+	-	-	+	-	-	-
CYP3A4 substrate	-	+	+	-	+	+	+	+	+
CYP inhibitory promiscuity	-	+	-	-	+	+	+	+	-
Hepatotoxicity	+	-	-	-	-	-	-	-	-
Human Ether-a-go-go-Related Gene inhibition	-	+	-	-	-	+	-	+	+
Human Intestinal Absorption	+	+	+	+	+	+	+	+	+
Human oral bioavailability	+	-	+	-	+	-	-	+	-
Mitochondrial toxicity	-	+	+	+	+	+	+	+	+
Nephrotoxicity	+	-	-	-	-	-	-	-	+
Acute Oral Toxicity	1.927911	2.682666	2.564216	1.584643	2.853549	2.025461	2.574924	2.573651	0.93410
P-glycoprotein inhibitior	-	+	+	-	-	+	-	+	-
P-glycoprotein substrate	-	+	-	-	+	+	+	-	+
Plasma protein binding	0.90996	0.761109	0.921986	0.419808	0.529639	0.956002	0.720404	0.830053	0.82829
Reproductive toxicity	+	+	+	+	+	+	+	+	+
Respiratory toxicity	-	+	+	+	+	+	+	+	+
Subcellular localzation	Plasma membrane	Mitochondria	Mitochondria	Nucleus	Mitochondria	Mitochondria	Mitochondria	Mitochondria	Mitocho
UGT catelyzed	-	-	-	+	-	-	-	-	-

Models	Tafamids	Leumateprone	Bromperidol	L-DOPA	Meloperone	Pimozide	Azabuperone	Anisolpirol	Deuterab
Water solubility	-4.55183	-3.38666	-4.00928	-1.66278	-2.79501	-3.70658	-3.40819	-2.24233	-3.19399

Conclusion

PARKIN loss of function has been disclosed to be implicated in Parkinson's disease and at the moment no available small molecule to activate or increase the activity of this gene. However, this current study has revealed the effectiveness of antineuropsychiatric/antipsychotic drugs as potential activators of PARKIN in the treatment of PD, and lumateperone was revealed to be the most promising candidate for interacting with PARKIN. In this regard, lumateperone may be further subjected to in vitro or in vivo study to explore its activity as a potential activator of PARKIN.

Declarations

Conflicts of interest

The authors declare that they have no conflicts of interest

Acknowledgments

The authors sincerely appreciate the contribution of Dr. Amos O. Abolaji of the Department of Biochemistry, University of Ibadan to the success of this study.

Source of funding

This research did not receive any specific grant from funding agencies in the public, commercial, or not-for-profit sectors.

Authors' contribution

Conceptualization: A. Ibrahim, and N. Ipinloju. Introduction and Methodology: A. Ibrahim, A. Ipinloju. Data curation and formal analysis: A. Ibrahim, and N. Ipinloju. Writing original draft preparation: A. Ibrahim and N. Ipinloju. Writing review and editing: S. A. Muhammad, A. Ibrahim, N. Ipinloju. O. E. Oyeneyin and Supervision: S. A. Muhammad and . O. E. Oyeneyin. All authors read and approve the final manuscript

ORCID

Abdulwasiu Ibrahim https://orcid.org/0000-0003-3456-005X

Nureni Ipinloju https://orcid.org/0000-0002-2683-7146

Sulieman Alhaji Muhammad https://orcid.org/0000-0003-2421-3556

Oluwatoyin Emmanuel Oyeneyin https://orcid.org/0000-0001-5709-0244

References

1. Marino, S., Ciurleo, R., Di Lorenzo, G., Barresi, M., De Salvo, S., Giacoppo, S., & Bramanti, P. (2012). Magnetic resonance imaging markers for early diagnosis of Parkinson's disease. *Neural regeneration research*, *7*(8), 611
2. Dauer, W., & Przedborski, S. (2003). Parkinson's disease: mechanisms and models. *Neuron*, *39*(6), 889–909
3. Bekris, L. M., Mata, I. F., & Zabetian, C. P. (2010). The genetics of Parkinson disease. *Journal of geriatric psychiatry and neurology*, *23*(4), 228–242
4. Quinn, P. M., Moreira, P. I., Ambrósio, A. F., & Alves, C. H. (2020). PINK1/PARKIN signalling in neurodegeneration and neuroinflammation. *Acta neuropathologica communications*, *8*(1), 1–20
5. Papapetropoulos, S., Adi, N., Ellul, J., Argyriou, A. A., & Chroni, E. (2007). A prospective study of familial versus sporadic Parkinson's disease. *Neurodegenerative diseases*, *4*(6), 424–427
6. Lücking, C. B., Dürr, A., Bonifati, V., Vaughan, J., De Michele, G., Gasser, T., & Brice, A. (2000). The European Consortium on Genetic Susceptibility in Parkinson's Disease, The French Parkinson's Disease Genetics Study Group. Association between early-onset Parkinson's disease and mutations in the parkingene. *New England Journal Of Medicine*, *342*(21), 1560–1567
7. Dawson, T. M. (2006). Parkin and defective ubiquitination in Parkinson's disease.*Parkinson's Disease and Related Disorders*,209–213
8. Corti, O., Lesage, S., & Brice, A. (2011). What genetics tells us about the causes and mechanisms of Parkinson's disease.*Physiological reviews*
9. Moore, D. J. (2006). Parkin:a multifaceted ubiquitin ligase
10. Antonini, A., Odin, P., Pahwa, R., Aldred, J., Alobaidi, A., Jalundhwala, Y. J., & Chaudhuri, K. (2021). The long-term impact of levodopa/carbidopa intestinal gel on 'off'-time in patients with advanced Parkinson's disease: a systematic review. *Advances in Therapy*, *38*(6), 2854–2890
11. Prasad, E. M., & Hung, S. Y. (2021). Current therapies in clinical trials of Parkinson's disease: A 2021 update. *Pharmaceuticals*, *14*(8), 717
12. Kim, T. W. (2015). Drug repositioning approaches for the discovery of new therapeutics for Alzheimer's disease. *Neurotherapeutics*, *12*(1), 132–142
13. Rochais, C., Lecoutey, C., Gaven, F., Giannoni, P., Hamidouche, K., Hedou, D., & Dallemagne, P. (2015). Novel multitarget-directed ligands (MTDLs) with acetylcholinesterase (AChE) inhibitory and serotonergic subtype 4 receptor (5-HT4R) agonist activities as potential agents against Alzheimer's disease:

the design of donecopride. *Journal of medicinal chemistry*, *58*(7), 3172–3187

14. Nikolic, K., Mavridis, L., Djikic, T., Vucicevic, J., Agbaba, D., Yelekci, K., & Mitchell, J. B. (2016). Drug design for CNS diseases: polypharmacological profiling of compounds using cheminformatic, 3D-QSAR and virtual screening methodologies. *Frontiers in neuroscience*, *10*, 265
15. Schrödinger, L. (2018). *Schrödinger Release 2018-1: Maestro*. Schrödinger LLC: New York, NY, USA
16. Oyeneyin, O. E., Odadawo, S. O., Orimoloye, S. M., Akintemi, E. O., Ipinloju, N., Asere, A. M., & Owolabi, T. O. (2021). Prediction of inhibition activity of BET bromodomain inhibitors using grid search based extreme learning machine and molecular docking. *Lett Drug Des Discov*, *18*, 1–11
17. Madhavi Sastry, G., Adzhigirey, M., Day, T., Annabhimoju, R., & Sherman, W. (2013). Protein and ligand preparation: parameters, protocols, and influence on virtual screening enrichments. *Journal of computer-aided molecular design*, *27*(3), 221–234
18. Oyeneyin, O. E., Abayomi, T., Ipinloju, N., Agbaffa, E., Akerele, D., & Arobadade, O. (2021). Investigation of Amino Chalcone Derivatives as Anti-Proliferative Agents against MCF-7 Breast Cancer Cell Lines-DFT, Molecular Docking and Pharmacokinetics Studies.*Advanced Journal of Chemistry-Section A*.4:288–299
19. Friesner, R. A., Murphy, R. B., Repasky, M. P., Frye, L. L., Greenwood, J. R., Halgren,T. A., … Mainz, D. T. (2006). Extra precision glide: Docking and scoring incorporating a model of hydrophobic enclosure for protein – ligand complexes. *Journal of medicinal chemistry*, *49*(21), 6177–6196
20. Balogun, T. A., Ipinloju, N., Abdullateef, O. T., Moses, S. I., Omoboyowa, D. A., James, A. C., Saibu, O. A., Akinyemi, W. F., & Oni, E. A. (2021). Computational Evaluation of Bioactive Compounds from Colocasia affinis Schott as Novel EGFR inhibitor for Cancer Treatment. *Cancer Informatics*, *20*, 1–12
21. Oyeneyin, O. E., Adejoro, I. A., Obadawo, B. S., Amoko, J. S., Kayode, I. O., Akintemi, E. O., et al. (2021). Investigation into the molecular properties of 3-(4-hydroxyphenyl) prop-2-en-1 one 4- phenyl Schiff base and some of its derivativesDFT and Molecular Docking studies. Sci Lett 2021; 9(1), 4–11
22. Shao, Y., Molnar, L. F., Jung, Y., et al. (2014). *SPARTAN '14, build 1.01*. Irvine (CA): Wavefunction Inc.
23. Oyeneyin, O. E., Adejoro, I. A., Obadawo, B. S., Amoko, J. S., Kayode, I. O., Akintemi, E. O., et al. (2021). Investigation into the molecular properties of 3-(4-hydroxyphenyl) prop-2-en-1 one 4- phenyl Schiff base and some of its derivativesDFT and Molecular Docking studies. Sci Lett 2021; 9(1), 4–11
24. Becke, A. D. (1993). Density-functional thermochemistry. III. The role of exact exchange. *The Journal Of Chemical Physics*, *98*(7), 5648–5652
25. Oyeneyin, O. E., Ojo, N. D., Ipinloju, N., et al. (2022). Investigation of Corrosion Inhibition Potentials of Some Aminopyridine Schiff Bases Using Density Functional Theory and Monte Carlo Simulation. *Chemistry Africa*, *5*:, 319–332
26. Jensen, F. (2021). Polarization consistent basis sets: Principles. *The Journal Of Chemical Physics*, *115*(20), 91139125
27. Koopmans, T. (1934) Über ydie zuordnung von wellenfunktionen und eigenwerten zu den einzelnen elektroneneines atoms.Physica1,104–113
28. Oprea, T. I., Bauman, J. E., Bologa, C. G., Buranda, T., Chigaev, A., Edwards, B.S., … Sklar, L. A. (2011). Drug repurposing from an academic perspective. *Drug Discovery Today: Therapeutic Strategies*, *8*(3–4), 61–69
29. Lee, H. M., & Kim, Y. (2016). Drug repurposing is a new opportunity for developing drugs against neuropsychiatric disorders. *Schizophrenia research and treatment*, *2016*
30. AL-Makhzumi, Q. M. A. H., Abdullah, H. I., & AL-Ani, R. R. (2018). Theoretical study of N-Methyl-3-phenyl-3-(-4-(Trifluoromethyl)phenoxy)propan as a Drug and its Five Derivatives. *Journal of Biosciences and Medicines*, *6*, 80–98
31. Geerlings, P., & De Proft, F. (2002). Chemical Reactivity as Described by Quantum Chemical Methods. *International Journal of Molecular Sciences*, *3*(4), 276–309
32. Oyeneyin, O., Ipinloju, N., Ojo, N., & Akerele, D. (2021). Structural Modification of Ibuprofen as new NSAIDs via DFT, Molecular Docking and Pharmacokinetics Studies. *JEPS*, *33*(4), 614–626
33. Chakraborty, T., Gazi, K., & Ghosh, D. C. (2010). Computational of the atomic radii through the conjoint action of the effective nuclear charge and ionization energy. *Molecular Physics*, *108*(16), 2081–2092
34. Nasiri, S. K., Reisi-Vanani, A., & Hamadanian, M. (2018). Molecular Structure, Spectroscopic, Local and Global Reactivity Descriptors and NBO Analysis of C32H12: A New Buckybowl and Sub- Fullerene Structure, Polycyclic Aromat. *Compd*, *40*(3), 693–704
35. Chattaraj, P. K., Perez, P., Zevallos, J., & Toro-Labbe, A. (2002). Theoretical study of the trans N2H2→ cis-N2H2 and F2S2→ FSSF reactions in gas and solution phases. *J Mol Struct THEOCHEM*, *580*(1–3), 171–182
36. Wanat, K. (2020). Biological barriers, and the influence of protein binding on the passage of drug across them. *Molecular Biology Reports*, *47*, 3221–3231
37. Smith, D., Di, L., & Kerns, E. (2010). The effect of plasma protein binding on in vivo efficacy: misconceptions in drug discovery. *Nature Reviews. Drug Discovery*, *9*(12), 929–939
38. McDonnel, A. M., & Dang, C. H. (2013). Basic review of the cytochrome p450 system. *Journal of the advanced practitioner in oncology*, *4*(4), 263
39. Walum, E. (1998). Acute oral toxicity. *Environmetal health perspectives*, *106*, 497–503
40. Mortelmans, K. (2000). Zeiger EjMrf, mutagenesis mmo. The Ames salmonella/microsome mutagenicity assay. *Mutation Research*, *455*, 29–60
41. Savjani, K. T., Gajjar, A. K., & Savjani, J. K. (2012). Drug solubility: Importance and enhancement techniques. ISRN pharm. 2012: 195727
42. Lamothe, S. M., Guo, J., Li, W., Yang, T., & Zhang, S. (2016). The human ether-a-go-go-related gene (hERG) potassium channel represents an unusual target for protease-mediated damage. *Journal of biological science*, *291*(39), 20387–20401

Tables

Table 1 and 3 are available in the Supplementary Files section.

Figures

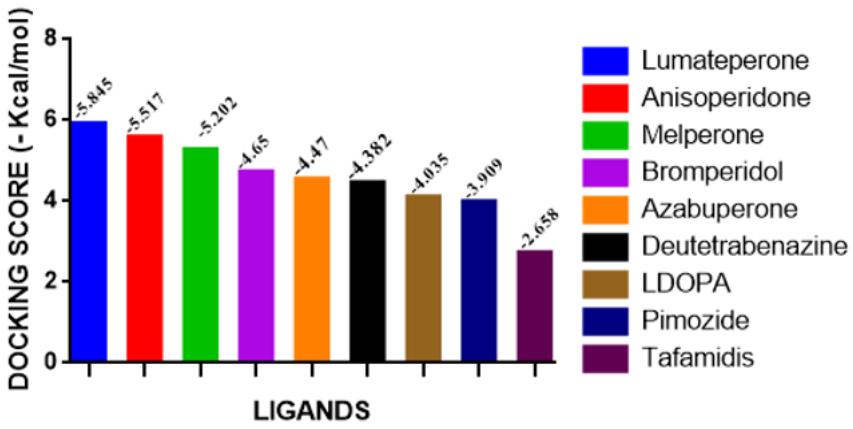

Figure 1

Docking score (Binding Affinity) of the docked ligands against PARKIN Protein

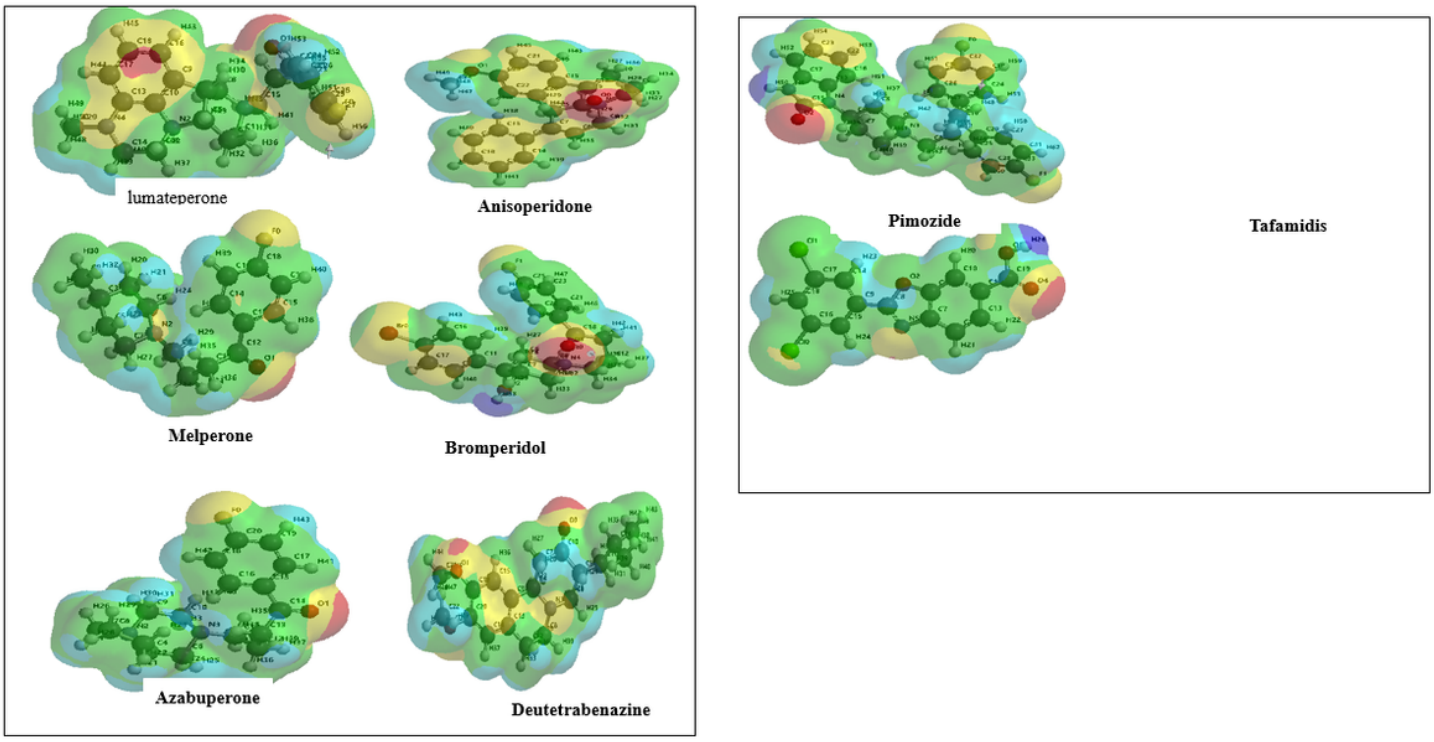

Figure 2

MEP map of the studied compounds

Supplementary Files

This is a list of supplementary files associated with this preprint. Click to download.

- Table1and3.docx